

Received:
23 May 2018Revised:
11 October 2018Accepted:
15 October 2018<https://doi.org/10.1259/bjr.20180466>

Cite this article as:

Meyer J, Eley J, Schmid TE, Combs SE, Dendale R, Prezado Y. Spatially fractionated proton minibeam. *Br J Radiol* 2019; **92**: 20180466.

SMALL ANIMAL IGRT SPECIAL FEATURE: REVIEW ARTICLE

Spatially fractionated proton minibeam

¹JUERGEN MEYER, PhD, ²JOHN ELEY, PhD, ^{3,4,5}THOMAS E SCHMID, PhD, ^{3,4,5}STEPHANIE E COMBS, MD, ⁶REMI DENDALE, MD and ⁷YOLANDA PREZADO, PhD

¹Department of Radiation Oncology, University of Washington, Seattle, WA, USA

²Department of Radiation Oncology, School of Medicine, University of Maryland, Baltimore, MD, USA

³Department of Radiation Oncology, Klinikum rechts der Isar, Technische Universität München (TUM), München, Germany

⁴Department of Radiation Sciences (DRS), Institute of Innovative Radiotherapy (IRT), Helmholtz Zentrum München, Neuherberg, Germany

⁵Deutsches Konsortium für Translationale Krebsforschung (DKTK), Partner Site Munich, Heidelberg, Germany

⁶Institut Curie, Centre de Protonthérapie d'Orsay, Orsay, France

⁷Laboratoire d'Imagerie et Modélisation en Neurobiologie et Cancérologie (IMNC), Centre National de la Recherche Scientifique, Universités Paris 11 and Paris 7, Campus d'Orsay, Orsay, France

Address correspondence to: Dr Juergen Meyer

E-mail: juergen@uw.edu

ABSTRACT

Extraordinary normal tissue response to highly spatially fractionated X-ray beams has been explored for over 25 years. More recently, alternative radiation sources have been developed and utilized with the aim to evoke comparable effects. These include protons, which lend themselves well for this endeavour due to their physical depth dose characteristics as well as corresponding variable biological effectiveness. This paper addresses the motivation for using protons to generate spatially fractionated beams and reviews the technological implementations and experimental results to date. This includes simulation and feasibility studies, collimation and beam characteristics, dosimetry and biological considerations as well as the results of *in vivo* and *in vitro* studies. Experimental results are emerging indicating an extraordinary normal tissue sparing effect analogous to what has been observed for synchrotron generated X-ray microbeams. The potential for translational research and feasibility of spatially modulated proton beams in clinical settings is discussed.

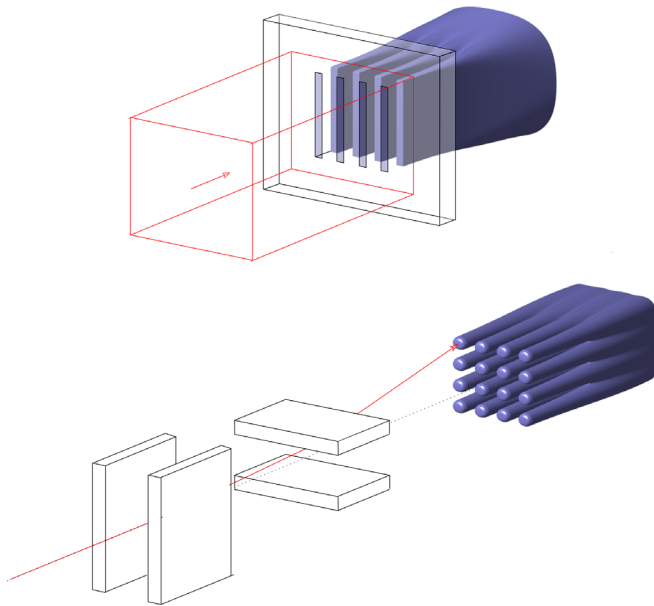
INTRODUCTION

Technological advances in radiation delivery and treatment planning have notably improved the shaping of high dose regions to the surface of tumour volumes and this conformal precision also reduces dose to organs-at-risk.¹ However, treatments of tumours close to sensitive structures, such as the central nervous system, as well paediatric cancers are still compromised by the upper tolerance dose of normal tissue structures. Finding novel approaches that reduce normal tissue damage is of utmost importance. This is the case for the utilization of distinct spatial dose distributions, commonly referred to as spatially fractionated radiation therapy (SFRT). In SFRT, irradiation is performed by using highly spatially modulated beams, as illustrated in [Figure 1](#). The dose profiles on the beam entrance side consist of peaks and valleys in contrast to homogeneous profiles in standard radiation therapy (RT). The beams may be spatially fractionated in one or two directions, referred to as micro/minibeams ([Figure 1a](#)) and GRID ([Figure 1b](#)), respectively. The concept of SFRT was first introduced in 1909 by German physician, Alban Köhler,^{2,3} to achieve better skin sparing for deep seated tumours. The value of GRID

or Sieve therapy for the treatment of difficult cases without risk of skin necrosis was further reported in the 1950s.⁴⁻⁷ The advent of megavoltage beams for RT, providing higher penetration and better skin sparing, resulted in SFRT to be consigned to oblivion for several decades. GRID therapy was “rediscovered” in the 1970s using Co-60 units^{8,9} and later in the 1990s by using megavoltage beams provided by medical linear accelerators (linacs).¹⁰ Linac-based grid therapy is still in use at a few hospitals in the USA, recently also with clinical proton beams,^{11,12} to deliver large, single fraction doses to patients with bulky tumours to shrink or palliate the disease with minimum damage to normal tissues.¹³⁻¹⁸

In parallel developments, pre-clinical research was carried out by Curtis, Zeman and co-workers¹⁹⁻²¹ at Brookhaven National Laboratory, starting in 1959, in the context of studies on the possible biological effects of cosmic radiation. They observed a highly non-linear inverse relationship between radiosensitivity and tissue volume exposed. The experiment they conducted involved irradiation of mouse brains with a deuteron beam of varying sizes and

Figure 1. Illustration of spatially fractionated proton beams that produce a uniform dose at depth. (a) multiplanar beams generated with a collimator and (b) pencil beams generated with steering magnets.



doses. The tolerance dose criterion was the onset of cavitation, defined as histologic lesion 24 days after exposure. For the 1 mm, 75 μm and 25 μm wide beams, cavitation was observed after 250, 750 and extraordinarily high 10,000 Gy, respectively.¹⁹ For the 25 μm beam, doses of 4000 Gy were needed to produce death of nerve and glial cells. This was accompanied, however, by an intact overall tissue architecture and no permanent blood vessels damage.^{20,21} Three decades later, Slatkin and colleagues, also from Brookhaven National Laboratory, decided to further exploit these early observations. Along with the advent of third-generation synchrotron sources providing kilovoltage X-ray beams with negligible beam divergence and high brilliance, they proposed microbeam radiation therapy (MRT).^{22,23} The use of perfectly parallel beams results in a pattern of peaks and valleys that remain fairly constant with tissue depth.^{23–25} This contrasted with the relatively rapid degradation of the grid patterns with depth of the first grid therapies. The promise was that extraordinary normal tissue sparing could be maintained well below the skin level. This was indeed repeatedly confirmed, with most experiments concentrating on the effects of MRT on the central nervous system in several animal models.^{25–33} Doses as high as 600 Gy delivered with microscopic beams were well-tolerated without signs of radionecrosis but maintenance of the overall tissue architecture and permanence of apparently normal vessels in the path of the microbeams. MRT has also been shown, despite extremely heterogeneous dose distributions, to delay tumour growth and in some cases induce tumour ablation in different kinds of tumours in rodents.^{34–40}

The need for ultra-high dose rates ($>100 \text{ Gy s}^{-1}$) to prevent blurring by cardiosynchronous pulsations⁴¹ of the peak and valleys patterns, the need for low-kilovoltage energies ($<200 \text{ keV}$),⁴² and the technical challenges related to positioning and

dosimetry triggered the exploration of minibeam radiation therapy (MBRT)^{29,43} with slightly larger but still submillimetre beams. MBRT is less vulnerable to beam smearing than MRT,^{44,45} technically easier to implement and feasible with higher energies.⁴² MBRT has also been shown to significantly increase the normal tissue resistance in animal experiments with respect to uniform irradiation,^{46–50} while delaying tumour growth.^{46,51}

The inherent advantages of charged particle beams in RT use along with the increasing accessibility of proton therapy centres has prompted the consideration of the synergies between spatial dose fractionation and the use of protons.^{52–60} Termed proton minibeam radiation therapy (pMBRT), it offers several intrinsic dosimetric advantages over X-ray-based MBRT, including the distinct radiobiological properties of protons,⁶¹ and the possibility of producing uniform dose at depth, while maintaining modulation on the beam entrance side. The biological evaluations performed to date confirm a remarkable reduction in normal tissue toxicity^{53,60,62} even with supramillimetre beams.⁶²

The aim of this work is to review the developments on pMBRT since the first publications in 2013. This includes the technical aspects and dosimetric considerations as well as an overview of the beam parameters at different facilities that have been utilized to date. This is followed by a review of published radiobiology experiments as well as considerations for a common framework to describe and report dose from spatially fractionated beams. The final part of the paper discusses future developments and potential for translational research.

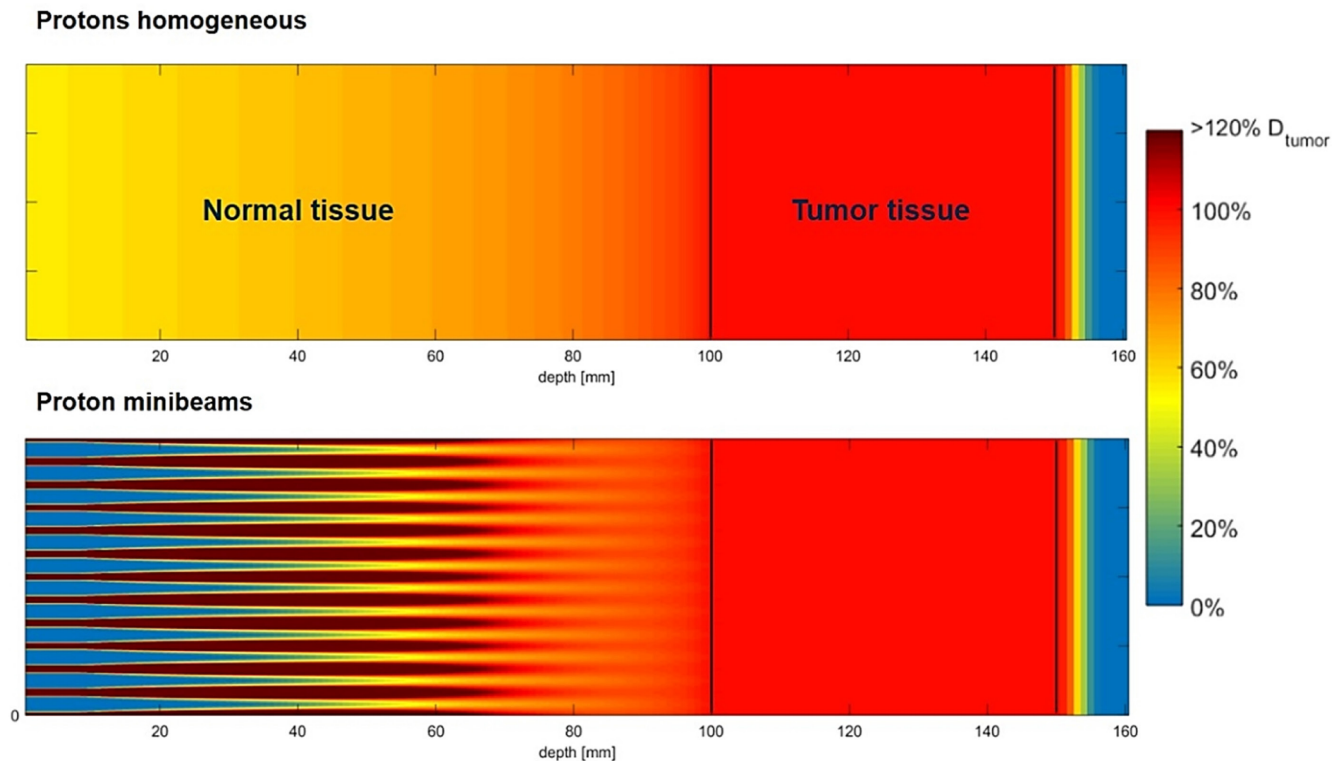
TECHNICAL ASPECTS

Proton minibeam arrays can be generated similarly to synchrotron generated microbeams by shaping a broad beam into multiplanar arrays by means of a multislit collimator,^{52,55,58,59} as illustrated in Figure 1a. In contrast to the 25–100 μm -wide kilovoltage MRT beams, characteristically spaced 200–400 μm , MBRT typically uses $\geq 300 \mu\text{m}$ wide beams with on-centre distance reaching from twice the width to 3.5 mm. An alternative approach, shown in Figure 1b, is pencil beam scanning, whereby an array of proton pencil beams is sequentially placed at defined distances to form a grid pattern of high and low dose regions.⁵³ Both approaches are henceforth referred to as proton minibeam arrays.

Beam design considerations

Proton minibeam arrays and proton grid therapy have a distinct dosimetric advantage over X-ray-based spatially modulated beams in that a uniform dose can be delivered at the depth of the Bragg peak (BP) even if merely a single beam direction is used. This fundamentally distinguishes pMBRT from X-ray GRID therapies, where typically non-uniform dose in the tumour is used with the aim to debulk large tumours. For a proton the energy loss along its path is inversely proportional to the square of the proton's velocity, becoming a relatively large energy loss just before stopping. For a beam of protons, this results in a dose build up toward the end of the proton beam range that is laterally spread out due to multiple coulomb scattering along the proton beam path. Due to its small area dimension, a single minibeam in isolation may not exhibit a large BP. But by strategically placing

Figure 2. Concept of proton minibeam. Simulated dose distributions with spread out Bragg peak for (a) homogeneous broad beam (top) and (b) minibeam (bottom) irradiation. Figure adapted from Sammer et al⁶³ with permission.



adjacent minibeam at an appropriately calculated distance, their lateral scattering dose clouds at the end of the proton range can be overlapped to result in a reconstituted large BP providing a laterally continuous uniform peak dose distribution at depth, while also maintaining high spatial beam modulation on the entrance side.⁵⁹ This is depicted in Figure 2, which illustrates the difference between a uniform and non-uniform pMBRT beam, both with spread-out BP. pMBRT contrasts with X-ray-based MBRT, in which at least two orthogonal interlaced planar arrays are required to generate uniform dose at depth, leading to a more complex and error prone irradiation geometry. On the other hand, one of the drawbacks for very narrowly collimated proton beams is that the BP to entrance dose ratio becomes smaller than unity due to the reduction in in-scatter leading to a loss of charged particle equilibrium, which negates the inherent physical advantage of dose deposition of protons with depth. Further details of this phenomenon can be found in, *e.g.* Hong et al.⁶⁴ Therefore, minibeam widths $>300 \mu\text{m}$ are desirable to maintain a reasonable entrance to BP ratio.⁵⁶

The incident proton beam energy and the type of beam collimation determine the proton beam spectrum and hence the penetration characteristic of the proton minibeam. The peak beam energy dictates the depth of the BP and the energy distribution about the peak determines the sharpness of the distal dose falloff. The distance between incident minibeam governs the peak-to-valley dose ratio (PVDR) and the degree of dose overlap between individual BPs. For collimator generated minibeam, the position of the collimator relative to the irradiation object has a strong influence on the PVDR.^{57,65} For instance, retracting

a pMRT multislit collimator from a water phantom by 2 cm reduced the PVDR by a factor of 10, from 37 to 3.7 in one study,⁵⁷ indicating the complexity of the dosimetry. A further factor is the collimator material in combination with the collimator position, which governs the amount of neutron contribution to the irradiation object, which was quantified by several authors^{57,65,66} and discussed in several commentaries^{52,67,68} and further below.

Feasibility of uniform target irradiation

Prezado et al first considered the use of proton minibeam in 2013 in their GATE/Geant4⁶⁹ Monte Carlo simulation study,⁵⁹ in which they simulated two proton energies, 105 MeV and 1 GeV. They concluded that similar or higher PVDR compared to MBRT can be achieved, with penumbras sharper than that of a GammaKnife beam. They also evaluated an interlaced arrangement for the higher energy beam to obtain a uniform dose in the target. The same team implemented pMBRT at a clinical centre (Institut Curie Centre de Protonthérapie d'Orsay) in 2014⁵⁸ by using mechanical collimators.^{58,65}

In 2013, Dollinger and co-authors⁶⁰ took advantage of the beam widening at the distal end of parallel proton beams to obtain a uniform dose in the tumour. In their pioneering experiment with a 20 MeV proton beam on a human skin model, described further below, their irradiation geometry resembled a lattice with 10–50 μm wide microchannels spaced 500 μm apart. They concluded that proton microchannel irradiation maintains cell viability and reduces inflammatory responses and genetic damage compared to homogeneous irradiation.

Dilmanian et al,⁵² one of the early pioneers of microbeam radiotherapy, conducted Monte Carlo simulations with MCNPX⁷⁰ in 2015 to investigate the beam characteristics of a multislit collimator generated 109 MeV proton minibeam to produce a uniform dose on a clinical particle facility. They considered both pencil beam scanning and used a 5 cm thick tungsten collimator with 300 μm beam width and 1 mm on-centre spacing.

Lee et al⁵⁵ used TOPAS⁷¹ Monte Carlo simulations to systematically optimize their pMBRT collimator design for a preclinical 50.5 MeV proton beam line in 2016. They also obtained a slit width of 300 μm with 1 mm on-centre spacing as an optimal configuration to obtain a uniform dose at depth. For the collimator material, iron was suggested instead of tungsten because of the considerably lower neutron yield at that energy. They further investigated the trade-offs between different collimator thicknesses and the resulting PVDR. They concluded that ideally the collimator should be made thicker than theoretically necessary to stop the beam to achieve sharp penumbras and high modulation. However, this is at cost of a drop in dose rate with collimator thickness.

In similar work, investigating collimator material and optimizing their existing collimator geometry of 400 μm with a centre-on distance of 3.2 mm for a 100 MeV beam, Guardiola et al⁶⁵ concluded that although the neutron yield of a tungsten collimator is up to three times higher than that of other materials, the overall neutron dose contribution is less than 1% and therefore negligible. Nonetheless, uncertainties in the relative biological effectiveness (RBE) of neutrons remain a concern,⁶⁸ in particular in the valley regions. This is because the valley dose is thought to be the determining factor for normal tissue tolerance.⁷² Alternative materials that have been proposed to reduce the neutron dose by approximately 30% include nickel, iron and brass.⁷³

The most sophisticated framework to obtain optimal irradiation geometry was recently presented by Sammer et al.⁶³ They defined the incident beam geometry and energy within an elegant inverse planning approach and evaluated the effectiveness of different beam geometries in terms of survival fractions. The overall aim was to optimize the geometry and distances between the minibeam to minimize overall cell killing outside the target, while maintaining uniform dose coverage at depth. Opposed to previous work, this was achieved by utilizing the linear quadratic (LQ) model instead of dose-based optimization. The difference being that the LQ model incorporates the characteristic non-linear cell killing behaviour with increasing dose. Planar and both square and hexagonal lattice arrangements were considered for the incoming beam geometry. Optimisation was carried out for clinical proton beam energies with spread-out-BPs and realistic tumour depths. They concluded that pencil beams, in particular in a hexagonal arrangement, were superior to planar beam geometry, in terms of minimising normal tissue damage and treatment delivery efficiency. These findings highlight the limitations of merely dose-based optimization of minibeam arrangements. They further suggest that future clinical implementation should focus on pencil proton beams rather

than on planar proton minibeam to maximize the efficacy of spatial fractionation

Dosimetry

Dosimetry of SFRT beams is intrinsically challenging due to the narrow dimensions of the high spatial modulation. For absolute dosimetry, the gold-standard in RT are ionization chambers, which do not have the spatial resolution to resolve the peak and valley regions. Therefore, film dosimetry is the main option for both absolute and relative dosimetry,^{52,58} with cross calibrated diamond detectors with a 1 μm sensitive detector layer as an alternative option.⁵⁷ Another option is a scintillation detector which can count individual protons.⁵³ With regard to Gafchromic films, Peucelle et al successfully corrected for film saturation using EBT3 film.⁵⁸ They provided a detailed uncertainty budget for their approach and estimated a combined uncertainty of 4%, consisting of individual uncertainties resulting from absolute dose determination with an ionization chamber, optical density readout and film calibration. Gafchromic films are also known to exhibit a linear energy transfer (LET) dependence and this becomes relevant for proton dosimetry, especially when lower energy protons are present.⁷⁴ These lower energy protons are primarily near the BP and in the valley regions as a result of in-scatter within the collimator channels, the latter of which can lead to an underestimation of the valley dose. The energy dependence manifests itself with an under response with depth and reaches a maximum towards the end of the proton range. The magnitude of the Gafchromic EBT film underresponse can amount to 20–30% at the peak of the Bragg curve^{58,75} or even >30% below 50 MeV.⁷⁶ Cao et al⁷⁶ characterised the under-response of EBT3 film by comparing it with ion chamber and microdiamond detector measurements and corresponding Monte Carlo simulations to determine a film calibration curve as a function of depth and hence LET. The energy dependence as a function of LET was found to be highly non-linear within the uncertainties of film positioning and statistical uncertainties of the simulations. This highlights that to obtain reproducible results careful film calibration with regard to dose and spectral characterisation by means of Monte Carlo simulations⁵⁷ are recommended.

Operational proton minibeam

Currently, there are four facilities that have implemented and delivered proton minibeam and are actively conducting research. They are groups in Orsay, France, the Technical University in Munich, Germany, the University of Maryland/MD Anderson, USA and the University of Washington in Seattle, USA. A summary of the beam details is given in [Table 1](#).

The first implementation of pMBRT was achieved in 2014⁵⁸ at the Institut Curie—Centre de Protonthérapie d'Orsay, a clinical proton therapy facility. A 230 MeV proton cyclotron (IBA, Belgium) delivers the beam to a universal nozzle-equipped gantry and two horizontal beamlines. In a first phase, proton minibeam were generated with mechanical collimators^{58,65} with 400 and 700 μm -width and on-centre distances of 3200 and 3500 μm , respectively. The beam geometries were chosen to obtain a quasi-homogeneous dose distribution in the target while

Table 1. Overview of the beam parameters used by different groups

Author	Location	Beam energy (MeV)	Collimator material/ thickness	Slit/channel width (μm)	Spacing (μm)	Approx. dose rate (Gy/min)
Prezado <i>et al.</i> (2013)	Orsay	105 1 GeV	Brass/ 5 cm & magnetic lead/ 70 cm & magnetic	700 700	1400, 2800, 3500 1400, 2800, 3500	-
Dollinger <i>et al.</i> (2013)	Munich	20	PBS	10–50	500	40–100
Girst <i>et al.</i> (2015)	Munich	20	PBS	260–520	1800	40–100
Dilmanian <i>et al.</i> (2015)	MD Anderson	109	Tungsten/ 5 cm	300	1000	90
Peucelle <i>et al.</i> (2015)	Orsay	100	Brass/ 5 cm	400 700	3200 3500	2
Lee <i>et al.</i> (2016), Meyer <i>et al.</i> (2017)	Seattle	50.5	Steel/ 2.5 cm	300	1000	10–20
Guardiola <i>et al.</i> (2017)	Orsay	100	Brass, tungsten, nickel, iron	400	3200	6
Prezado <i>et al.</i> (2017)	Orsay	100	Brass/5 cm	400 (1100 in rat)	3200	2
Mossahebi <i>et al.</i> (2017)	Maryland	80–140	Tungsten/5 cm	300	1000	90
de Marzi <i>et al.</i> (2018)	Orsay	123 150	PBS	400 (1100 in rat)	1000	6

PBS, pencil beam scanning;

retaining sufficient spatial fractionation in normal tissue.⁵⁹ The first series of biological studies⁶² confirmed the main working hypothesis: pMBRT provides a remarkable gain in normal tissue sparing. Recently pMBRT was implemented on a pencil beam scanning system,⁷⁷ obtaining a dose rate of 6 Gy min⁻¹ in the central minibeam at the BP position. Further optimization with the goal of obtaining an adequate dose rate to be able to treat patients within a reasonable time frame of a few minutes are ongoing.

Accelerator Laboratory SNAKE, Munich, Germany
At SNAKE (Supraleitendes Nanoskop für angewandte Kernenergie-Experimente), a large variety of biological experiments have been performed on a regular basis since 1970. It is a Tandem accelerator of the “Emperor” (MP) series and manufactured by High Voltage Engineering Corporation, located at the Accelerator Laboratory at the TUM campus in Garching. The scanning ion microprobe delivers focused ion beams with sub micrometre irradiation accuracy, enabling irradiation of, *e.g.* cell nuclei with single or tallied ions. Details of the facility can be found elsewhere.^{78–80} For pMBRT, a 20 MeV proton beam is focused or collimated to a submillimetre beam size and translated such that tissue between the minibeam receive nearly zero dose. For mouse irradiations a specially developed, temperature-controlled aluminium holder was developed.⁵³ For *in vivo* dosimetry, every proton hitting a scintillator-photomultiplier detector positioned directly in the beam path can be counted, such that

the dose to any area can be accurately calculated. The LET of the proton beam on the surface is 2.7 keV μm^{-1} and the range of protons in water is <5 mm.⁵³

The University of Texas MD Anderson Cancer Center (MDACC, Houston, TX) and University of Maryland School of Medicine (Baltimore, MD)
In 2013, a collaboration was formed by Dilmanian, Krishnan and Eley to investigate the potential of proton minibeam therapy and to begin experimental testing with high-energy protons using a clinical system and a tungsten multi slit collimator.⁵² Initial work was carried out on the Hitachi PROBEAT synchrotron accelerator (Tokyo, Japan) at the MD Anderson Proton Therapy Center, Houston, TX. A 100 MeV proton beam was utilized in combination with a 5 cm tungsten multislit collimator producing 300 μm planar proton minibeam with 1 mm on-centre spacing, resulting in a 23:1 PVDR. The initial results established that proton minibeam therapy is feasible on existing clinical proton therapy facilities and it was concluded that the approach could achieve low-enough valley doses to expect tissue sparing effects. In further work by the group, a small animal irradiation platform was constructed at the Maryland Proton Treatment Center, using optical components and precision translation stages.⁸¹ On the Varian Medical Systems ProBeam superconducting cyclotron accelerator (Palo Alto, CA), pencil beams are available to generate proton minibeam with a collimator of the same

specifications as previously used at MD Anderson. Measured PVDR for proton energies of 80, 100, 120, and 140 MeV were 25 ± 5 , 31 ± 3 , 20 ± 2 , and 15 ± 2 .⁸¹

University of Washington, Seattle, USA

The University of Washington developed the first image-guided experimental small animal platform to investigate radiobiological effects of proton beams.⁸² The heart of the facility is a Scanditronix MC50 cyclotron, which was installed in 1983 for fast neutron therapy,⁸³ for which it is still used clinically. One of the fixed neutron beamline room was converted in 2012 to a research proton beamline with a maximum energy of 50.5 MeV. The beamline is fully integrated into an X-ray small animal irradiator (SARRP, Xstrahl Ltd, Camberley, Surrey, UK), with high resolution cone beam CT. The proton beam is near monoenergetic and produces a pristine BP between 7 and 21 mm depth. To produce a proton minibeam with a uniform dose at depth, a 25 mm thick multislit steel collimator with 300 μm slit width and 1 mm on-centre spacing is utilized.⁵⁵ A full dosimetric characterization of the beam, including LET, energy spectrum, and RBE on a per voxel based was recently carried out.⁵⁷

BIOLOGICAL WORKS

3D human skin model

First experimental evidence demonstrating reduced negative irradiation effects of microchannel irradiation with protons compared with homogeneous broad beam irradiation⁶⁰ was conducted in 2013 at SNAKE in Munich. The investigation was carried out on a commercially available *in vitro* three-dimensional (3D) human skin model (Epiderm FT⁺, MatTek Corporation, Ashland, MA, USA) to account for the preserved 3D geometric arrangement and communication of cells present in tissues *in vivo*. The skin model was used as a target system for assessing micronucleus induction to get a non-animal skin-based genotoxicity assay.⁸⁴ The skin was chosen as an example for an acute side effect since acute radiation dermatitis is common in RT and occurs during or after the end of radiotherapeutic treatment. Despite improvements in technology that have greatly reduced the burden of cutaneous reactions, radiation dermatitis remains an important side effect. Even today, approximately 85% of patients will experience skin reaction in the exposed area.⁸⁵

In an *in vitro* study,⁶⁰ greater cell viability and lower cytogenetic damage was demonstrated using the MTT (3-(4,5-dimethylthiazol-2-yl)-2,5-diphenyltetrazolium bromide) tissue viability and micronuclei assays, with a reduced and shorter inflammatory response, measured as the release of inflammatory cytokines in the culture medium of the skin.

The aim of a second study was to compare synchrotron generated X-ray beams at the European Synchrotron Radiation Facility in Grenoble, France, and proton microbeam irradiation at SNAKE and to compare the effects of increasing minibeam width on potential side effects in normal tissue.⁸⁶ 20-MeV protons minibeam with a $\sigma = 260$ and 520 μm and interchannel distance of 1.8 mm were applied to a 3D human skin model and compared to homogeneous proton irradiation. A significant reduction of cytogenetic damage was observed for the widened minibeam

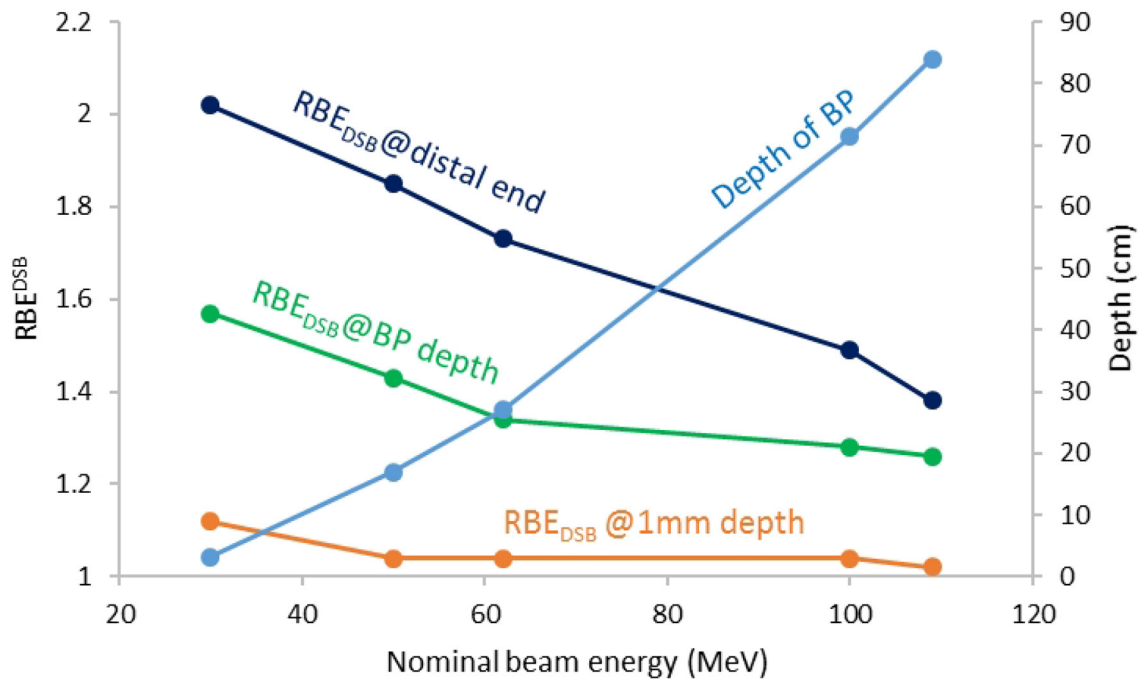
compared to homogeneous irradiation. For homogeneously overlapping minibeam, the cytogenetic damage did not exceed that of homogeneous irradiation.⁸⁶ Normal tissue irradiation with either X-ray or proton minibeam maintained a higher cell viability and DNA integrity compared to homogeneous irradiation, and thus might improve normal tissue protection after RT.

Small animal studies

Most of the small animal work to date has been carried out on normal tissue sparing. As the goal of proton minibeam generally is to deliver a uniform dose to the target, it is assumed that tumour response is no different to when a broad beam is used to deliver the same homogeneous dose. This is different to GRID irradiation, which is used clinically to debulk large tumours, for which the goal is to deliver high dose peaks, rather than a uniform dose (see, e.g.¹¹). Clinically relevant proof-of-concept results can only be obtained using proton minibeam irradiation in an animal model where the complexity of irradiation effects, including the response of vasculature and immune system, can be analysed. In the study by Girst et al,⁵³ the acute side effects of proton minibeam irradiation were compared to those of conventional homogeneous proton irradiation of the normal tissue in a validated mouse model. Mouse ears were chosen as a model for murine skin due to the small ear thickness of only about 250 μm , which allowed the detection of 20 MeV protons directly behind the ears. Visible reactions resulting from irradiation were categorized as erythema, desquamation and changes of ear morphology and hair loss. While homogeneous irradiation with 60 Gy induced an up to fourfold increase in the ear thickness and a high degree of oedema in both skin layers, no swelling could be detected at any time-point after minibeam irradiation at the same mean dose. Likewise, no erythema or desquamation or hair loss was visible in the mice that were irradiated with the proton minibeam compared to those that received a homogeneous proton irradiation. Histological analysis supported these findings by showing no changes for minibeam-irradiated ears, but a significant enlargement of the epidermis at the time of the highest ear swelling together with large inflammatory and necrotic regions after homogeneous irradiation. The results from this animal study clearly demonstrated that proton minibeam irradiation reduces the incidence of acute side effects compared with conventional broad beam irradiation in a mouse ear model.

Prezado et al performed the first long-term evaluation of the effects of pMBRT on normal brain.⁶² Fischer 344 rats ($n = 8$ per study arm) were exposed to 100-MeV protons with integral doses of 25 Gy, using either solid beams or planar minibeam with 1.1 mm minibeam widths and 3.2 mm on-centre spacing. Minibeam peak doses were 58 Gy and the PVDR was 6.5:1 at 1 cm depth, with an effective mean dose of 25 Gy. Animals were followed for up to 6 months after irradiation. A longitudinal MRI study was carried out along with histological analysis. Rats treated with conventional proton irradiation exhibited severe moist desquamation and substantial brain damage. In contrast, no significant damage was observed in the pMBRT group.⁶² These results demonstrate that pMBRT leads to remarkable gain in normal tissues tolerances in delicate and treatment limiting organs, like the central nervous system. This opens the door for a

Figure 3. Comparison of the RBE_{DSB} (left axis) at different depths for different nominal proton beam energies simulated on the University of Washington research proton beamline. The depth of the BP is shown on the right axis. BP, Bragg peak.



more efficient treatment of highly radio-resistant tumours, such as high-grade gliomas (GBM).

The Orsay team has recently also shown that pMBRT leads to considerable tumour control in glioma-bearing rats with significantly reduced toxicity. It was shown that tumour sterilization can be achieved even with highly heterogeneous dose distributions⁸⁷ and more work is currently under way to confirm these findings.

RBE and EUD considerations

One of the pertinent endeavours to ensure that experimental results in SFRT are reproducible, is to have a framework that allows to account for the differences between the spatially fractionated beams used at different institutions. Currently, no commonly agreed reporting standards or metrics exist to compare mini-/microbeams of different geometries (*i.e.* on-centre spacing, slit width), dose modulation (*i.e.* valley dose, PVDR), beam type and energy (*i.e.* X-rays, protons, carbon ions) and dose rates (*i.e.* 2–10000 Gy min⁻¹). Meyer et al⁵⁷ proposed to include RBE and equivalent uniform dose (EUD) considerations to account for beam type and energy as well as beam modulation. They simulated the RBE for double strand breaks (DSB) for the different proton beam energies of the institutions mentioned in "Operational proton minibeam" and found differences in RBE_{DSB} of over 25% at the BP and close to 50% at the distal end of the BP. On the beam entrance side, the differences were less than 10% for nominal proton beam energies between 30 and 109 MeV. This is illustrated in Figure 3. They further found that the effect of the collimator on the RBE weighted dose was minimal with regard to both the peaks and valleys. In terms of the EUD, which is based on the

well-established LQ model for cell survival, it was shown that in most situations the mean dose is not as previously thought a suitable quantity to compare spatially fractionated and uniform beam geometries, although this has historically often been used for experimental comparisons to demonstrate the benefits of SFRT. The reason for the discrepancy between mean dose and EUD is because cell kill is not a linear function of dose whereas the mean dose is. In particular, the higher the dose the further the EUD trends toward the valley dose.⁸⁸ This reflects observations from MBRT experiments, for which typically high doses in the order of tens or hundreds of Grays are used. It is generally assumed that the toxicity is more dependent on valley region parameters rather than the peak dose.⁷² Several studies investigating partial volume irradiation with split beams and the effects of low dose baths support this observation.^{49,50,89} Possible explanations for the increased efficacy of spatially fractionated beams include in-field bystander effects,⁹⁰ cytokines⁴⁹ and differential modulation of immune and inflammatory gene pathways.⁹¹

RBE and EUD models have known limitations and have not yet been verified experimentally for highly spatially modulated dose distributions. Nevertheless, incorporating known responses, such as spatially varying RBE and EUD, are an important step toward inter-institutional reproducibility of experimental results. Thus, the findings from these models should not be considered in absolute terms but rather as a means to help interpret past findings, prospectively explore trends and to design future experiments. Biological effects that cannot be accounted for with these models, such as the difference in beam geometries and dose rate, need to be further explored and may help identify possible explanations for the overall phenomena related to micro-/minibeams. Further refinements and validation of the biological models and

metrics for spatially modulated dose distributions are required (see, e.g.⁹²⁻⁹⁴).

FUTURE

The ultimate goal is to translate and reproduce the findings from small animal experiments into the clinic. The spatial fractionation patterns in pMBRT strongly depend on the beam energy, which is a function of the depth of the irradiation target. This will require higher beam energies and, as each small proton beamlet widens with depth, the on-centre spacing between adjacent minibeamlets will become considerably larger, which in itself is an advantage in terms of normal tissue sparing. However, on most current clinical proton beam facilities, the smallest beam spots available are several millimetres in diameter, depending on the beam energy, and therefore much larger than what is expected to elicit an extraordinary normal tissue sparing as described here within. For robustness and to reduce the peak entrance doses more than one beam direction will most likely have to be considered. Several feasibility studies with multiple beams and interlaced beam arrangements have been published⁹⁵⁻⁹⁸ in this regard. While these planning feasibility studies use beam dimensions that are not comparable to pMBRT, they provide an insight into some of the practical obstacles that will have to be overcome for successful clinical translation. In addition, even with the larger dimensions of current clinical pencil beams, an EUD effect can be expected, especially for high fraction doses,⁵⁷ which could in itself provide a worthwhile advantage.

Although the physical characteristics of proton therapy are well-understood, the biological aspects, particularly the complex biological endpoints for normal tissue complications, have been less explored in a systematic way. RBEs obtained from traditional endpoints, such as clonogenic cell kill, are likely to have limited applicability to assess proton action on multiscale endpoints, such as cancer progression, tumour control and carcinogenesis risk. In-depth and systematic proton radiobiology evaluations, including the assessment on how protons act on multicellular processes, such as angiogenesis, are essential for the optimization of proton radiotherapy. The limited access to beam time and the lack of an adequate image-guidance for small animal treatment at clinical facilities create the need for the development of more precision preclinical small animal proton therapy facilities. The availability of such facilities will allow advancement in animal-based proton RT research, thereby providing new insights into the biological responses of proton vs photon irradiations and helping to optimise the treatment protocols. The possibility of performing systematic and comprehensive experiments would help unravel the distinct biological mechanisms participating when spatial dose fractionation is used.

From a clinical perspective, SFRT may be the next step forward in precision radiation medicine. Through the dose reduction to normal tissue outside the entry channel of the narrow beam setup, the anticipated damage to normal tissue and subsequently the risk for treatment-related side effects may be reduced significantly. At the same time, the total dose to the tumour can be increased. Especially for radiation resistant tumours, this may enhance local tumour control following the dose-response

curves well characterized for most tissues, while not increasing overall rates of side effects.

Another interesting area of future work is to combine and separate out the magnitude of the sparing effects of spatial fractionation and ultra-high dose rate irradiation. The latter is referred to as FLASH irradiation⁹⁹ and uses dose rates in the order of 100 Gy s⁻¹.¹⁰⁰ While spatial fractionation has been shown to produce normal tissue sparing effects on its own, combining spatial fractionation with FLASH irradiation may or may not amplify this effect and might help to shed some light in the underlying biology governing the biological processes leading to tissue sparing.

Overall, two clinical approaches can be followed for SFRT: (1) Reduction of changes to normal tissue with comparable local control in diseased tissue or (2) comparable changes to normal tissue and thus identical rates of side effects, but higher dose to the tumour and thus improvement of outcome. From an oncological perspective, both strategies are worthwhile following depending on the tumour type evaluated. Patients with low-risk tumours with long-term survival might benefit more from reduction of side effects, thus Strategy 1; this group might include lymphomas, low-grade gliomas or benign lesions such as meningioma. Patients with radiation resistant tumours, such as osteosarcoma, chordoma or chondrosarcoma, will mostly benefit from Strategy 2, since local control is still not satisfactory.

While proton minibeamlets have shown the potential for a paradigm shift in radiation treatment, clinical trials are required to confirm the results from small animal experiments in humans. One of the challenges will be to determine revised normal tissue tolerance doses for spatially fractionated irradiation. As this is a function of the irradiation geometry, the dose, and in some cases the orientation of the beam relative to the functional subunits of a certain organ, this is no trivial task. The first therapeutic trials should evaluate the dose toxicity relationship and should be Phase I studies. They could include primitive brain tumours with a very poor prognosis, such as tumours which are inoperable with imprecise limits and are resistant to radiotherapy. Another indication could be total brain irradiation for multiple brain metastases.

The possibility of radiation-induced abscopal effects provides the opportunity to test the association with some medical treatments like targeted therapies such as anti-PD1. Lymphocytes are known as the most radiosensitive cells in the mammalian body¹⁰¹ and the idea behind the potential immunogenic effects of SFRT is the fact that in conventional uniform tumour irradiation tumour infiltrating lymphocytes are eliminated with each daily fraction, whereas spatially fractionated irradiation can be designed to partially spare tumour infiltrating lymphocytes in or near the tumour, allowing the opportunity to induce a systemic response. Phase II studies will then need to be conducted to determine the dose and antitumoral efficacy relationship according to the tumour type and its tissue environment.

In addition to cancer treatment, the high-precision of SFRT could be used for functional radiation treatments,⁵⁹ such as

trigeminal neuralgia, treatment of epilepsy or other neurological diseases such as Parkinsonism. Experimental setups have shown that MRT to the hippocampus can deliver a highly precise dissection, without any radiation-induced oedema or radionecrosis 3 months after irradiation.¹⁰² Histological analysis showed a very well preserved hippocampal cytoarchitecture and confirmed the presence of clear-cut microscopic transections across the hippocampus. Earlier experiments had shown that tissue dissection with microbeams might be effective in epilepsy treatment due to cortical transections.^{103,104}

CONCLUSIONS

Proton minibeam is a relatively new concept and currently, only a few facilities worldwide have the technical capabilities to deliver pMBRT beams. Opposed to classical X-ray GRID therapy, pMBRT can also deliver a uniform dose to the target

while at the same time maximizing the beam modulation along the proximal beam path. First encouraging experimental results from small animal studies are emerging but in order for this new technology to be successfully translated into the clinic, interinstitutional reproducibility of the results should be a high priority. This can only be achieved through meticulous dosimetry and following recommended reporting standards.^{57,105,106} In the long run, the generation of proton minibeam by means of magnetically focussed pencil beams will provide the most convenient and versatile approach for clinical implementation and will allow the widespread availability of proton minibeam. Apart from the technological requirements, characterisation of the dose response of normal tissue to different flavours of pMBRT and categorization of the biological mechanism will be the most challenging part of the endeavour on the road to clinical implementation.

REFERENCES

- Garibaldi C, Jereczek-Fossa BA, Marvaso G, Dicuonzo S, Rojas DP, Cattani F, et al. Recent advances in radiation oncology. *Eccancermedicalscience* 2017; **11**: 785. doi: <https://doi.org/10.3332/ecancer.2017.785>
- Köhler A. Theorie einer Methode, bisher unmöglich unanwendbar hohe Dosen Röntgenstrahlen in der Tiefe des Gewebes zur therapeutischen Wirksamkeit zu bringen ohne schwere Schädigung des Patienten, zugleich eine Methode des Schutzes gegen Röntgenverbrennung überhaupt. *Fortschr Geb Roentgenstr* 1909; **14**: 27–9.
- Laissue JA, Blattmann H, Slatkin DN, Köhler A. Inventor of grid therapy. *Z Med Phys* 1874-19472012; **22**: 90–9.
- Freid JR, Lipman A, Jacobson LE. Roentgen therapy through a grid for advanced carcinoma. *Am J Roentgenol Radium Ther Nucl Med* 1953; **70**: 460–76.
- Jolles B, Russ S. *X-ray Sieve Therapy in Cancer. A Connective Tissue Problem*. Boston: Little Brown Company; 1953.
- Marks H. A new approach to the roentgen therapy of cancer with the use of a grid. *J Mt Sinai Hosp N Y* 1950; **17**: 46–8.
- Tenzel WV. Experience with grid therapy. *Radiology* 1952; **59**: 399–408. doi: <https://doi.org/10.1148/59.3.399>
- Barkova AM, Kholin VV. Theoretical calculation of the spatial distribution of a Co 60 gamma radiation dose field under a grid. *Med Radiol* 1971; **16**: 64–70.
- Muth CP, Salewski D, Glaser FH, Heider KM. Grid method in telecobalt therapy (author's transl. *Radiobiol Radiother* 1977; **18**: 691–9.
- Mohiuddin M, Curtis DL, Grizos WT, Komarnicky L. Palliative treatment of advanced cancer using multiple nonconfluent pencil beam radiation. A pilot study. *Cancer* 1990; **66**: 114–8. doi: [https://doi.org/10.1002/1097-0142\(19900701\)66:1<114::AID-CNCR2820660121>3.0.CO;2-L](https://doi.org/10.1002/1097-0142(19900701)66:1<114::AID-CNCR2820660121>3.0.CO;2-L)
- Gao M, Mohiuddin MM, Hartsell WF, Pankuch M, Fractionated S. Spatially fractionated (GRID) radiation therapy using proton pencil beam scanning (PBS): Feasibility study and clinical implementation. *Med Phys* 2018; **45**: 1645–53. doi: <https://doi.org/10.1002/mp.12807>
- Farr JB, Moskvina V, Lukose RC, Tuomanen S, Tsiamas P, Yao W. Development, commissioning, and evaluation of a new intensity modulated minibeam proton therapy system. *Med Phys* 2018; **45**: 4227–37. doi: <https://doi.org/10.1002/mp.13093>
- Mohiuddin M, Fujita M, Regine WF, Megooni AS, Ibbott GS, Ahmed MM, et al. GRID): a new paradigm in the management of advanced cancers. *International journal of radiation oncology, biology, Physics* 1999; **45**: 721–7.
- Narayanasamy G, Zhang X, Meigooni A, Paudel N, Morrill S, Maraboyina S, et al. Therapeutic benefits in grid irradiation on Tomotherapy for bulky, radiation-resistant tumors. *Acta Oncol* 2017; **56**: 1043–7. doi: <https://doi.org/10.1080/0284186X.2017.1299219>
- Peñagaricano JA, Moros EG, Ratanatharathorn V, Yan Y, Corry P. Evaluation of spatially fractionated radiotherapy (GRID) and definitive chemoradiotherapy with curative intent for locally advanced squamous cell carcinoma of the head and neck: initial response rates and toxicity. *Int J Radiat Oncol Biol Phys* 2010; **76**: 1369–75. doi: <https://doi.org/10.1016/j.ijrobp.2009.03.030>
- Reiff JE, Huq MS, Mohiuddin M, Suntharalingam N. Dosimetric properties of megavoltage grid therapy. *Int J Radiat Oncol Biol Phys* 1995; **33**: 937–42. doi: [https://doi.org/10.1016/0360-3016\(95\)00114-3](https://doi.org/10.1016/0360-3016(95)00114-3)
- Zwicker RD, Meigooni A, Mohiuddin M. Radiobiological advantage of megavoltage grid therapy. *Int J Radiat Oncol Biol Phys* 2001; **51**: 401. doi: [https://doi.org/10.1016/S0360-3016\(01\)02562-7](https://doi.org/10.1016/S0360-3016(01)02562-7)
- Neuner G, Mohiuddin MM, Vander Walde N, Goloubeva O, Ha J, Yu CX, et al. High-dose spatially fractionated GRID radiation therapy (SFGRT): a comparison of treatment outcomes with Cerrobend vs. MLC SFGRT. *Int J Radiat Oncol Biol Phys* 2012; **82**: 1642–9. doi: <https://doi.org/10.1016/j.ijrobp.2011.01.065>
- Zeman W, Curtis HJ, Gebhard EL, Haymaker W. Tolerance of mouse-brain tissue to high-energy deuterons. *Science* 1959; **130**: 1760–1. doi: <https://doi.org/10.1126/science.130.3391.1760-a>
- Zeman W, Curtis HJ, Baker CP. Histopathologic effect of high-energy-particle microbeams on the visual cortex of the mouse brain. *Radiat Res* 1961; **15**: 496–514. doi: <https://doi.org/10.2307/3571293>
- Curtis HJ. The use of deuteron microbeam for simulating the biological effects of heavy cosmic-ray particles. *Radiat Res Suppl* 1967;

- 7: 250–7. doi: <https://doi.org/10.2307/3583718>
22. Slatkin DN, Spanne P, Dilmanian FA, Gebbers JO, Laissue JA. Subacute neuropathological effects of microplanar beams of X-rays from a synchrotron wiggler. *Proc Natl Acad Sci U S A* 1995; **92**: 8783–7. doi: <https://doi.org/10.1073/pnas.92.19.8783>
 23. Slatkin DN, Spanne P, Dilmanian FA, Sandborg M, Radiation-Therapy M. Microbeam radiation therapy. *Med Phys* 1992; **19**: 1395–400. doi: <https://doi.org/10.1118/1.596771>
 24. Martínez-Rovira I, Sempau J, Fernández-Varea JM, Bravin A, Prezado Y. Monte carlo dosimetry for forthcoming clinical trials in X-ray microbeam radiation therapy. *Phys Med Biol* 2010; **55**: 4375–88. doi: <https://doi.org/10.1088/0031-9155/55/15/012>
 25. Siegbahn EA, Stepanek J, Bräuer-Krisch E, Bravin A. Determination of dosimetrical quantities used in microbeam radiation therapy (MRT) with Monte Carlo simulations. *Med Phys* 2006; **33**: 3248–59. doi: <https://doi.org/10.1118/1.2229422>
 26. Bouchet A, Lemasson B, Le Duc G, Maisin C, Bräuer-Krisch E, Siegbahn EA, et al. Preferential effect of synchrotron microbeam radiation therapy on intracerebral 9L gliosarcoma vascular networks. *Int J Radiat Oncol Biol Phys* 2010; **78**: 1503–12. doi: <https://doi.org/10.1016/j.ijrobp.2010.06.021>
 27. Bouchet A, Serduc R, Laissue JA, Djonov V. Effects of microbeam radiation therapy on normal and tumoral blood vessels. *Physica Medica* 2015; **31**: 634–41. doi: <https://doi.org/10.1016/j.ejmp.2015.04.014>
 28. Dilmanian FA, Morris GM, Le Duc G, Huang X, Ren B, Bacarian T, et al. Response of avian embryonic brain to spatially segmented X-ray microbeams. *Cellular and Molecular Biology* 2001; **47**: 485–93.
 29. Dilmanian FA, Zhong Z, Bacarian T, Benveniste H, Romanelli P, Wang R, et al. Interlaced X-ray microplanar beams: A radiosurgery approach with clinical potential. *Proceedings of the National Academy of Sciences* 2006; **103**: 9709–14. doi: <https://doi.org/10.1073/pnas.0603567103>
 30. Laissue JA, Bartzsch S, Blattmann H, Bräuer-Krisch E, Bravin A, Dalléry D, et al. Response of the rat spinal cord to X-ray microbeams. *Radiotherapy and Oncology* 2013; **106**: 106–11. doi: <https://doi.org/10.1016/j.radonc.2012.12.007>
 31. Laissue JA, Blattmann H, Di Michiel M, Slatkin DN, Lyubimova N, Guzman R, et al. The weanling piglet cerebellum: a surrogate for tolerance to MRT (microbeam radiation therapy) in pediatric neuro-oncology. *Penetrating Radiation Systems and Applications Iii* 2001; **4508**: 65–73.
 32. Serduc R, van de Looij Y, Francony G, Verdonck O, van der Sanden B, Laissue J, et al. Characterization and quantification of cerebral edema induced by synchrotron X-ray microbeam radiation therapy. *Phys Med Biol* 2008; **53**: 1153–66. doi: <https://doi.org/10.1088/0031-9155/53/5/001>
 33. Zhong N, Morris GM, Bacarian T, Rosen EM, Avraham Dilmanian F, Dilmanian FA. Response of rat skin to high-dose unidirectional x-ray microbeams: a histological study. *Radiat Res* 2003; **160**: 133–42. doi: <https://doi.org/10.1667/3033>
 34. Bouchet A, Bräuer-Krisch E, Prezado Y, El Atifi M, Rogalev L, Le Clec'h C, et al. Better efficacy of synchrotron spatially microfractionated radiation therapy than uniform radiation therapy on glioma. *Int J Radiat Oncol Biol Phys* 2016; **95**: 1485–94. doi: <https://doi.org/10.1016/j.ijrobp.2016.03.040>
 35. Dilmanian FA et al. Response of rat intracranial 9L gliosarcoma to microbeam radiation therapy. *Neuro Oncol* 2002; **4**: 26–38. doi: <https://doi.org/10.1215/15228517-4-1-26>
 36. Dilmanian FA, Morris GM, Zhong N, Bacarian T, Hainfeld JF, Kalef-Ezra J, et al. Murine EMT-6 carcinoma: High therapeutic efficacy of microbeam radiation therapy. *Radiat Res* 2003; **159**: 632–41. doi: [https://doi.org/10.1667/0033-7587\(2003\)159\[0632:MECHTE\]2.0.CO;2](https://doi.org/10.1667/0033-7587(2003)159[0632:MECHTE]2.0.CO;2)
 37. Laissue JA, Geiser G, Spanne PO, Dilmanian FA, Gebbers J-O, Geiser M, et al. Neuropathology of ablation of rat gliosarcomas and contiguous brain tissues using a microplanar beam of synchrotron-wiggler-generated X rays. *Int J Cancer* 1998; **78**: 654–60. doi: [https://doi.org/10.1002/\(SICI\)1097-0215\(19981123\)78:5<654::AID-IJC21>3.0.CO;2-L](https://doi.org/10.1002/(SICI)1097-0215(19981123)78:5<654::AID-IJC21>3.0.CO;2-L)
 38. Miura M, Blattmann H, Bräuer-Krisch E, Bravin A, Hanson AL, Nawrocky MM, et al. Radiosurgical palliation of aggressive murine SCCVII squamous cell carcinomas using synchrotron-generated X-ray microbeams. *Br J Radiol* 2006; **79**: 71–5. doi: <https://doi.org/10.1259/bjr/50464795>
 39. Regnard P, Duc GL, Bräuer-Krisch E, Tropès I, Siegbahn EA, Kusak A, et al. Irradiation of intracerebral 9L gliosarcoma by a single array of microplanar x-ray beams from a synchrotron: balance between curing and sparing. *Phys Med Biol* 2008; **53**: 861–78. doi: <https://doi.org/10.1088/0031-9155/53/4/003>
 40. Serduc R, Bouchet A, Bräuer-Krisch E, Laissue JA, Spiga J, Sarun S, et al. Synchrotron microbeam radiation therapy for rat brain tumor palliation—influence of the microbeam width at constant valley dose. *Phys Med Biol* 2009; **54**: 6711–24. doi: <https://doi.org/10.1088/0031-9155/54/21/017>
 41. Poncet BP, Wedeen VJ, Weisskoff RM, Cohen MS. Brain parenchyma motion: measurement with cine echo-planar MR imaging. *Radiology* 1992; **185**: 645–51. doi: <https://doi.org/10.1148/radiology.185.3.1438740>
 42. Prezado Y, Thengumpallil S, Renier M, Bravin A. X-ray energy optimization in minibeam radiation therapy. *Med Phys* 2009; **36**: 4897–902. doi: <https://doi.org/10.1118/1.3232000>
 43. Prezado Y, Renier M, Bravin A. A new method of creating minibeam patterns for synchrotron radiation therapy: a feasibility study. *J Synchrotron Radiat* 2009; **16**: 582–6. doi: <https://doi.org/10.1107/S0909049509012503>
 44. Machado de Sola F, Vilches M, Prezado Y, Lallena AM. Impact of cardiosynchronous brain pulsations on Monte Carlo calculated doses for synchrotron micro- and minibeam radiation therapy. *Med Phys* 2018; **45**: 3379–. doi: <https://doi.org/10.1002/mp.12973>
 45. Eagle J, Meyer J, Marsh S. *Effect of micro-motion on proton mini-beams. EPSM 2016: Engineering and Physical Sciences in Medicine*. Sydney, Australia; 2016.
 46. Deman P, Vautrin M, Edouard M, Stupar V, Bobyk L, Farion R, et al. Monochromatic minibeam radiotherapy: from healthy tissue-sparing effect studies toward first experimental glioma bearing rats therapy. *Int J Radiat Oncol Biol Phys* 2012; **82**: e693–e700. doi: <https://doi.org/10.1016/j.ijrobp.2011.09.013>
 47. Prezado Y, Deman P, Varlet P, Jouvion G, Gil S, Le Clec'h C, et al. Tolerance to dose escalation in minibeam radiation therapy applied to normal rat brain: long-term clinical, radiological and histopathological analysis. *Radiat Res* 2015; **184**: 314–21. doi: <https://doi.org/10.1667/RR14018.1>
 48. Prezado Y, Dos Santos M, Gonzalez W, Jouvion G, Guardiola C, Heinrich S, et al. Transfer of minibeam radiation therapy into a cost-effective equipment for radiobiological studies: A proof of concept. *Sci Rep* 2017; **7**. doi: <https://doi.org/10.1038/s41598-017-17543-3>
 49. Bijl HP, van Luijk P, Coppes RP, Schippers JM, Konings AW, van der Kogel AJ. Unexpected changes of rat cervical spinal cord tolerance caused by inhomogeneous

- dose distributions. International journal of radiation oncology, biology. *Physics* 2003; **57**: 274–81.
50. van Luijk P, Bijl HP, Konings AWT, van der Kogel AJ, Schippers JM. Data on dose- volume effects in the rat spinal cord do not support existing NTCP models. International journal of radiation oncology, biology. *Physics* 2005; **61**: 892–900.
 51. Prezado Y, Sarun S, Gil S, Deman P, Bouchet A, Le Duc G. Increase of lifespan for glioma-bearing rats by using minibeam radiation therapy. *J Synchrotron Radiat* 2012; **19**: 60–5. doi: <https://doi.org/10.1107/S0909049511047042>
 52. Dilmanian FA, Eley JG, Krishnan S. Minibeam therapy with protons and light ions: physical feasibility and potential to reduce radiation side effects and to facilitate hypofractionation. *Int J Radiat Oncol Biol Phys* 2015; **92**: 469–74. doi: <https://doi.org/10.1016/j.ijrobp.2015.01.018>
 53. Girst S, Greubel C, Reindl J, Siebenwirth C, Zlobinskaya O, Walsh DWM, et al. Proton Minibeam Radiation Therapy Reduces Side Effects in an *In Vivo* Mouse Ear Model. *Int J Radiat Oncol Biol Phys* 2016; **95**: 234–41. doi: <https://doi.org/10.1016/j.ijrobp.2015.10.020>
 54. Henry T, Ureba A, Valdman A, Siegbahn A. Proton Grid Therapy: A Proof-of-Concept Study. *Technol Cancer Res Treat* 2017; **16**: 749–57. doi: <https://doi.org/10.1177/1533034616681670>
 55. Lee E, Meyer J, Sandison G. Collimator design for spatially-fractionated proton beams for radiobiology research. *Phys Med Biol* 2016; **61**: 5378–89. doi: <https://doi.org/10.1088/0031-9155/61/14/5378>
 56. Martínez-Rovira I, Fois G, Prezado Y. Dosimetric evaluation of new approaches in GRID therapy using nonconventional radiation sources. *Med Phys* 2015; **42**: 685–93. doi: <https://doi.org/10.1118/1.4905042>
 57. Meyer J, Stewart RD, Smith D, Eagle J, Lee E, Cao N, et al. Biological and dosimetric characterisation of spatially fractionated proton minibeam. *Physics in Medicine & Biology* 2017; **62**: 9260–81. doi: <https://doi.org/10.1088/1361-6560/aa950c>
 58. Peucelle C, Nauraye C, Patriarca A, Hierso E, Fournier-Bidoz N, Martínez-Rovira I, et al. Proton minibeam radiation therapy: Experimental dosimetry evaluation. *Med Phys* 2015; **42**: 7108–13. doi: <https://doi.org/10.1118/1.4935868>
 59. Prezado Y, Fois GR. Proton-minibeam radiation therapy: A proof of concept. *Med Phys* 2013; **40**: 031712. doi: <https://doi.org/10.1118/1.4791648>
 60. Zlobinskaya O, Girst S, Greubel C, Hable V, Siebenwirth C, Walsh DWM, et al. Reduced side effects by proton microchannel radiotherapy: study in a human skin model. *Radiat Environ Biophys* 2013; **52**: 123–33. doi: <https://doi.org/10.1007/s00411-012-0450-9>
 61. Girdhani S, Sachs R, Hlatky L. Biological Effects of Proton Radiation: What We Know and Don't Know. *Radiat Res* 2013; **179**: 257–72. doi: <https://doi.org/10.1667/RR2839.1>
 62. Prezado Y, Jouvion G, Hardy D, Patriarca A, Nauraye C, Bergs J, et al. Proton minibeam radiation therapy spares normal rat brain: Long-Term Clinical, Radiological and Histopathological Analysis. *Sci Rep* 2017; **7**. doi: <https://doi.org/10.1038/s41598-017-14786-y>
 63. Sammer M, Greubel C, Girst S, Dollinger G. Optimization of beam arrangements in proton minibeam radiotherapy by cell survival simulations. *Med Phys* 2017; **44**: 6096–104. doi: <https://doi.org/10.1002/mp.12566>
 64. Hong L, Goitein M, Bucciolini M, Comiskey R, Gottschalk B, Rosenthal S, et al. A pencil beam algorithm for proton dose calculations. *Phys Med Biol* 1996; **41**: 1305–. doi: <https://doi.org/10.1088/0031-9155/41/8/005>
 65. Guardiola C, Peucelle C, Prezado Y. Optimization of the mechanical collimation for minibeam generation in proton minibeam radiation therapy. *Med Phys* 2017; **44**: 1470–8. doi: <https://doi.org/10.1002/mp.12131>
 66. Lee E, Eagle J, Sandison G, Cao N, Stewart R, Marsh S, et al. SU-F-T-671: Effects of collimator material on proton minibeam. *Med Phys* 2016; **43**(6Part23): 3618–18. doi: <https://doi.org/10.1118/1.4956857>
 67. Dilmanian FA, Eley JG, Krishnan S. In reply to Sahadevan. *Int J Radiat Oncol Biol Phys* 2015; **93**: 1164–5. doi: <https://doi.org/10.1016/j.ijrobp.2015.08.051>
 68. Sahadevan Vet al. In regard to Dilmanian et al. *Int J Radiat Oncol Biol Phys* 2015; **93**: 1164. doi: <https://doi.org/10.1016/j.ijrobp.2015.08.052>
 69. Agostinelli S, Allison J, Amako K, Apostolakis J, Araujo H, Arce P, et al. Geant4—a simulation toolkit. *Nuclear Instruments and Methods in Physics Research Section A: Accelerators, Spectrometers, Detectors and Associated Equipment* 2003; **506**: 250–303. doi: [https://doi.org/10.1016/S0168-9002\(03\)01368-8](https://doi.org/10.1016/S0168-9002(03)01368-8)
 70. Pelowitz DB. MCNPX User's Manual. Version 2.7.0. In: *Laboratory LAN*; 2011.
 71. Perl J, Shin J, Schumann J, Faddegon B, Paganetti H. TOPAS: An innovative proton Monte Carlo platform for research and clinical applications. *Med Phys* 2012; **39**: 6818–37. doi: <https://doi.org/10.1118/1.4758060>
 72. Smyth LML, Senthil S, Crosbie JC, Rogers PAW. The normal tissue effects of microbeam radiotherapy: What do we know, and what do we need to know to plan a human clinical trial? *Int J Radiat Biol* 2016; **92**: 302–11. doi: <https://doi.org/10.3109/09553002.2016.1154217>
 73. Gustafsson B. *Optimization of Material in Proton-Therapy Collimators with Respect to Neutron Production*. Sweden: University of Uppsala; 2009.
 74. Perles LA, Mirkovic D, Anand A, Titt U, Mohan R. LET dependence of the response of EBT2 films in proton dosimetry modeled as a bimolecular chemical reaction. *Phys Med Biol* 2013; **58**: 8477–91. doi: <https://doi.org/10.1088/0031-9155/58/23/8477>
 75. Zhao L, Das JJ. Gafchromic EBT film dosimetry in proton beams. *Phys Med Biol* 2010; **55**: N291–N301. doi: <https://doi.org/10.1088/0031-9155/55/10/N04>
 76. Cao N, Ford E, Smith D, Saini J, Wootton L. S et al. eds. *Dosimetric Verification of Spatially-Modulated Proton Minibeam Profiles*. Nashville, TN; 2018.
 77. de Marzi L, Patriarca A, Guardiola C, Nauraye C, Dendale R, Prezado Y. Implementation of proton minibeam radiation therapy at a pencil beam scanning system. *Med Phys* submitted.
 78. Greubel C, Hable V, Drexler GA, Hauptner A, Dietzel S, Strickfaden H, et al. Competition effect in DNA damage response. *Radiat Environ Biophys* 2008; **47**: 423–9. doi: <https://doi.org/10.1007/s00411-008-0182-z>
 79. Greubel C, Hable V, Drexler GA, Hauptner A, Dietzel S, Strickfaden H, et al. Quantitative analysis of DNA-damage response factors after sequential ion microirradiation. *Radiat Environ Biophys* 2008; **47**: 415–22. doi: <https://doi.org/10.1007/s00411-008-0181-0>
 80. Schmid TE, Dollinger G, Hable V, Greubel C, Zlobinskaya O, Michalski D, et al. Relative biological effectiveness of pulsed and continuous 20MeV protons for micronucleus induction in 3D human reconstructed skin tissue. *Radiotherapy and Oncology* 2010; **95**: 66–72. doi: <https://doi.org/10.1016/j.radonc.2010.03.010>
 81. Mossahebi S, Snider J, Dilmanian F, Krishnan S, Eley J. Importance of secondary particles produced in a tungsten multislit

- collimator for proton minibeam therapy. *Med Phys* 2017; **44**: 2872–3.
82. Ford E, Emery R, Huff D, Narayanan M, Schwartz J, Cao N, et al. An image-guided precision proton radiation platform for preclinical *in vivo* research. *Phys Med Biol* 2017; **62**: 43–58. doi: <https://doi.org/10.1088/1361-6560/62/1/43>
 83. Moffitt GB, Jevremovic T, Stewart RD, Emery R, Sandison GA, Wootton LS, et al. Dosimetric characteristics and a historical perspective on the university of washington (UW) clinical neutron therapy system (CNTS). *Phys Med Biol* 2018;PMB-106753. R2, Accepted April 10th, 2018.
 84. Curren RD, Mun GC, Gibson DP, Aardema MJ. Development of a method for assessing micronucleus induction in a 3D human skin model (EpiDerm)[™]. *Mutation Research/Genetic Toxicology and Environmental Mutagenesis* 2006; **607**: 192–204. doi: <https://doi.org/10.1016/j.mrgentox.2006.04.016>
 85. Salvo N, Barnes E, van Draanen J, Stacey E, Mitera G, Breen D, et al. Prophylaxis and management of acute radiation-induced skin reactions: a systematic review of the literature. *Curr Oncol* 2010; **17**: 94–112.
 86. Girst S, Greubel C, Reindl J, Siebenwirth C, Zlobinskaya O, Dollinger G, et al. The influence of the channel size on the reduction of side effects in microchannel proton therapy. *Radiat Environ Biophys* 2015; **54**: 335–42. doi: <https://doi.org/10.1007/s00411-015-0600-y>
 87. Prezado Y, Gonzalez W, Patriarca A, Jouvion G, Nauraye C, Guardiola C, et al. PV-0569: Proton minibeam radiation therapy widens the therapeutic window for gliomas. *Radiotherapy and Oncology* 2018; **127**: S299–S300. doi: [https://doi.org/10.1016/S0167-8140\(18\)30879-X](https://doi.org/10.1016/S0167-8140(18)30879-X)
 88. Meyer J, Steward RD, Sandison G, Mayr N. *Does the equivalent uniform dose explain normal tissue sparing in spatially fractionated radiotherapy? Workshop on understanding high-dose, ultra-dose-rate and spatial fractionated radiotherapy*. Bethesda, Maryland: National Cancer Institute & Radiosurgery Society; 2018.
 89. van Luijk P, Pringle S, Deasy JO, Moiseenko VV, Faber H, Hovan A, et al. Sparing the region of the salivary gland containing stem cells preserves saliva production after radiotherapy for head and neck cancer. *Sci Transl Med* 2015; **7**: 305ra147. doi: <https://doi.org/10.1126/scitranslmed.aac4441>
 90. Kashino G, Kondoh T, Nariyama N, Umetani K, Ohigashi T, Shinohara K, et al. Induction of DNA double-strand breaks and cellular migration through bystander effects in cells irradiated with the slit-type microplanar beam of the spring-8 synchrotron. *International journal of radiation oncology, biology, Physics* 2009; **74**: 229–36.
 91. Bouchet A, Sakakini N, El Atifi M, Le Clec'h C, Brauer E, Moisan A, et al. Early gene expression analysis in 9L orthotopic tumor-bearing rats identifies immune modulation in molecular response to synchrotron microbeam radiation therapy8(12. *PLoS One* 2013; **8**: e81874. doi: <https://doi.org/10.1371/journal.pone.0081874>
 92. Peng V, Suchowska N, Esteves ADS, Rogers L, Claridge Mackonis E, Toohey J, et al. Models for the bystander effect in gradient radiation fields: Range and signalling type. *J Theor Biol* 2018; **455**: 16–25. doi: <https://doi.org/10.1016/j.jtbi.2018.06.027>
 93. Peng V, Suchowska N, Rogers L, Claridge Mackonis E, Oakes S, McKenzie DR. Grid therapy using high definition multileaf collimators: realizing benefits of the bystander effect. *Acta Oncol* 2017; **56**: 1048–59. doi: <https://doi.org/10.1080/0284186X.2017.1299939>
 94. Henríquez F, Castrillón S. A quality index for equivalent uniform dose. *J Med Phys* 2011; **36**: 126–32. doi: <https://doi.org/10.4103/0971-6203.83466>
 95. Lomax AJ, Schaer M. 322 INTENSITY MODULATED 'GRID' PROTON THERAPY. TRYING TO EXPLOIT 'SPATIAL FRACTIONATION' WITH PROTONS. *Radiotherapy and Oncology* 2012; **102**: S171–S173. doi: [https://doi.org/10.1016/S0167-8140\(12\)70282-7](https://doi.org/10.1016/S0167-8140(12)70282-7)
 96. Henry T, Ureba A, Valdman A, Siegbahn A. Proton Grid Therapy. *Technol Cancer Res Treat* 2016; **1533034616681670**: 1533034616681670. doi: <https://doi.org/10.1177/1533034616681670>
 97. Henry T, Bassler N, Ureba A, Tsubouchi T, Valdman A, Siegbahn A. Development of an interlaced-crossfiring geometry for proton grid therapy. *Acta Oncol* 2017; **56**: 1437–43. doi: <https://doi.org/10.1080/0284186X.2017.1350287>
 98. Tsubouchi T, Henry T, Ureba A, Valdman A, Bassler N, Siegbahn A. Quantitative evaluation of potential irradiation geometries for carbon-ion beam grid therapy. *Med Phys* 2018; **45**: 1210–21. doi: <https://doi.org/10.1002/mp.12749>
 99. Favaudon V, Caplier L, Monceau V, Pouzoulet F, Sayarath M, Fouillade C, et al. Ultrahigh dose-rate FLASH irradiation increases the differential response between normal and tumor tissue in mice. *Sci Transl Med* 2014; **6**: 245ra93. doi: <https://doi.org/10.1126/scitranslmed.3008973>
 100. Montay-Gruel P, Petersson K, Jaccard M, Boivin G, Germond J-F, Petit B, et al. Irradiation in a flash: Unique sparing of memory in mice after whole brain irradiation with dose rates above 100 Gy/s. *Radiotherapy and Oncology* 2017; **124**: 365–9. doi: <https://doi.org/10.1016/j.radonc.2017.05.003>
 101. Trowell OA. The sensitivity of lymphocytes to ionising radiation. *J Pathol Bacteriol* 1952; **64**: 687–704. doi: <https://doi.org/10.1002/path.1700640403>
 102. Fardone E, Pouyatos B, Bräuer-Krisch E, Bartzsch S, Mathieu H, Requardt H, et al. Synchrotron-generated microbeams induce hippocampal transections in rats. *Sci Rep* 2018; **8**: 184. doi: <https://doi.org/10.1038/s41598-017-18000-x>
 103. Romanelli P, Fardone E, Battaglia G, Bräuer-Krisch E, Prezado Y, Requardt H, et al. Synchrotron-generated microbeam sensorimotor cortex transections induce seizure control without disruption of neurological functions. *PLoS One* 2013; **8**: e53549. doi: <https://doi.org/10.1371/journal.pone.0053549>
 104. Studer F, Serduc R, Pouyatos B, Chabrol T, Bräuer-Krisch E, Donzelli M, et al. Synchrotron X-ray microbeams: A promising tool for drug-resistant epilepsy treatment. *Physica Medica* 2015; **31**: 607–14. doi: <https://doi.org/10.1016/j.ejmp.2015.04.005>
 105. Ford E, Deye J. Current instrumentation and technologies in modern radiobiology research-opportunities and challenges. *Semin Radiat Oncol* 2016; **26**: 349–55. doi: <https://doi.org/10.1016/j.semradonc.2016.06.002>
 106. Verhaegen F, Dubois L, Gianolini S, Hill MA, Karger CP, Lauber K, et al. ESTRO ACROP: Technology for precision small animal radiotherapy research: Optimal use and challenges. *Radiother Oncol* 2018; **126**: 471–8. doi: <https://doi.org/10.1016/j.radonc.2017.11.016>